Tracing apoptosis and stimulation in individual cells by fluorescence intensity and anisotropy decay

Dror Fixler
Bar-Ilan University
School of Engineering
Ramat-Gan 52900
Israel

Reuven Tirosh
Naomi Zurgil
Mordechai Deutsch
Bar-Ilan University
The Biophysical Interdisciplinary
   Jerome Schottenstein Center for the Research
   and the Technology of the Cellome
Physics Department
Ramat-Gan 52900
Israel

Abstract. Presented is the use of fluorescence lifetime (FLT), anisotropy decay, and associated parameters as differential indicators of cellular activity. A specially designed combination of a frequency mode based time resolved microscope and a picoliter well-per-cell array have been used to perform temporal measurements in individual cells under various biological conditions. Two biological models have been examined: mitogenic activation of peripheral blood mononuclear cells (PBMC) and induction of programmed cell death (apoptosis) in Jurkat T cells (JTC). The FLT of fluorescein stained PBMC was found to increase from 4 ± 0.02 to 4.5 ± 0.025 ns due to mitogenic activation, whereas during apoptosis in fluorescein stained JTC, the FLT remained constant. Notably, the rotational correlation times changed in both models: decreased in PBMC from 2.5 ± 0.08 to 2 ± 0.1 ns, and increased in JTC from 2.1 ± 0.07 to 3.3 ± 0.09 ns. FLT and rotational correlation time were used to calculate the steady state fluorescence anisotropy (FA) which was compared to directly measured FA values. The present study suggests that in addition to bioindication, the said parameters can provide valuable information about cellular mechanisms that may involve complex molecular diffusion dynamics, as well as information about structural changes that a cellular fluorophore undergoes in the course of cell activation. © *2005 Society of Photo-Optical Instrumentation Engineers.* [DOI: 10.1117/1.1924712]

Keywords: fluorescence lifetime (FLT); fluorescence intensity (FI); fluorescence anisotropy (FA); rotational correlation time; fluorescence anisotropy decay (FAD); frequency domain time resolved microscope (FDTRM).

Paper 04028 received Mar. 1, 2004; revised manuscript received Sep. 30, 2004; accepted for publication Dec. 1, 2004; published online Jun. 7, 2005.

1 Introduction

The present study introduces fluorescence anisotropy decay (FAD) and its associated parameters as a means for monitoring cellular activities, to achieve a more profound interpretation of events occurring in individual cells before and after biological manipulations.

One of the most powerful tools in cell research is fluorescence based cytometry.[1] Measurement of cell functionality is among its most significant and productive branches. The first functional parameter used was fluorescence anisotropy (FA, also denoted by r).[1] It was initially proposed by the Cerceks as an indicator of lymphocyte activation.[1] FA is considered to be an indicator of "long term biological alterations" as compared to "fast indicators" that monitor transient effects such as change in pH and membrane potential.[2,3]

Generally, FA of a fluorescent probe provides—in an extent much greater than its fluorescence intensity (FI)—valuable information about the environmental conditions of the media hosting that probe. According to the Perrin

equation[4] and its more convenient representation using anisotropy instead of polarization,[5] the steady-state FA of a distinct fluorescent molecular species undergoing rotational diffusion, is related to the fluorescence lifetime (FLT)—τ_F and to the rotational correlation time τ_R as follows:

$$\frac{r_0}{r} = 1 + \frac{\tau_F}{\tau_R} = 1 + \sigma, \qquad (1)$$

where r_0 is the FA of a "frozen gas like system" and is solely determined by the angle between the absorption and the emission transition dipole moments of the probe. The ratio τ_F / τ_R is defined as σ. Generally, τ_R is defined as the ratio $\eta V/RT$ (where η is the microenvironmental viscosity, V the molar volume of a spherical probe, R the gas constant, and T the absolute temperature). Thus, τ_R is the most dominant variable, reflecting environmental changes as monitored by FA. The more limited the rotational motion of the fluorescent probe, the higher the FA, and vice versa.

When monitoring cell functionality, cytometrists more frequently utilize FI rather than FA measurements. Nevertheless, unlike direct FI measurements, which are strongly dependent on nonrelevant variables (optical variables, light source insta-

Address all correspondence to Mordechai Deutsch, PhD, The Biophysical Interdisciplinary Schottenstein Center for the Research and the Technology of the Cellome, Physics Department, Bar-Ilan University, Ramat-Gan 52900, Israel. Tel: 972-3-5344675, 5318349, 5354148; Fax: 972-3-5342019; e-mail rtcellom@mail.biu.ac.il

bility, etc.), FA and the related parameters, τ_F and τ_R, are intrinsic, which in itself is a fortunate circumstance since it permits more reliable comparisons between data obtained from different experiments and different laboratories. Much more importantly, FAD allows for a deeper and more differential insight into steady state FA results. The emission of cellular probes, even of the same type, is heterogeneous due to the heterogeneous chemo-physical nature of the hosting cellular media, where the probes are distributed. The weight of each emitting group, its τ_F and τ_R values, may be best assessed via FAD measurements. Knowledge of these three variables provides a powerful means for understanding the mechanisms involved in FA alterations in general, and cellular/membranal changes in particular.

Briefly, the time dependences of $FI(t)$ and $r(t)$ are

$$FI(t) = I_0 \sum_{i=1}^{n} \alpha_i e^{-t/\tau_{F_i}},$$

$$\tag{2}$$

$$r(t) = r_0 \sum_{j=1}^{m} \beta_j e^{-t/\tau_{R_j}},$$

where $FI(t)$ is the instantaneous emission intensity comprised of n different decay components, $r(t)$ is the instantaneous FAD comprised of m different components and r_0 is the FAD immediately after excitation, at $t=0$. The steady state FA is obtained by integrating the intensity-weighted $r(t)$ over time:

$$\bar{r} = \int_0^{\infty} r(t) I(t) dt. \tag{3}$$

In the present study, an apparatus was designed and constructed, and a methodology was developed to permit measurements of steady state FA, as well as FLT and FAD, in individual cells in a population, before, during and after biological manipulations.

2 Materials and Methods

2.1 Materials

Phytohemagglutinin (PHA) (Wellcome Ltd., London, UK) was reconstituted in 5 mL of double-distilled water and further diluted 1:10. For stimulation, 0.1 mL of this solution was added to 1 mL cell suspension (final concentration 90 μg/mL). Fluorescein solutions (1, 5, 10, and 100 μM) were prepared by dissolving fluorescein (Sigma, St. Louis, MO, USA) in phosphate buffered saline (PBS) solutions having different pH (5, 6. 5, 7. 4, 8) and viscosity [different glycerol (Gly) PBS concentrations: 0, 30%, 60%, and 80% Gly]. Polyscience fluorescent beads of fluoresbrite (fluorescein), 5.7±0.1 μm in diameter, with low fluorescent intensity [2000–50 000 molecules of equivalent soluble fluorochromes (MESF)] were used, from Bangs Laboratories, Inc. (Fishers, IN, USA).

2.2 Cell Preparation

For separation of peripheral blood mononuclear cells (PBMC), 20 mL of heparinized blood, obtained from healthy volunteers, was diluted 1:1 in PBS, pH 7.2. Blood was then layered in a 10 mL density gradient solution (1.077 g/cm³, Ficol Paque, Pharmacia, Upsala, Sweden), and centrifuged at

550 g for 30 min. Cells accumulated at the interphase, between the plasma and ficol layers, were collected and washed three times with complete PBS and resuspended in PBS at a final concentration of 6×10^6 cells/mL. More than 70% of the cells were defined as T lymphocytes, and viability, determined by trypan blue exclusion, was always higher than 90%. Human Jurkat T-lymphoblast cell line was grown in a humidified atmosphere containing 5% CO_2, in a RPMI 1640 medium (Biological Industries, Beit Haemek, Israel), supplemented with 10% (v/v) heat inactivated fetal calf serum (Biological Industries, Beit Haemek, Israel), 2 mM L-glutamine, 10 mM HEPES buffer solution, 1 mM sodium pyruvate, 50 U/mL penicillin, and 100 μg/mL streptomycin.

2.3 Mitogenic Stimulation and Apoptosis Induction

Freshly prepared PBMC (10^7 cells/mL) were incubated at 37 °C with 90 μg/mL PHA for 45 min for mitogenic activation.

Apoptosis was induced by incubating Jurkat T-lymphoblast cells in complete RPMI 1640 medium in the presence of 50 μM H_2O_2 at 37 °C for various time periods, followed by a quick rinsing of the H_2O_2, to determine the initial time of the apoptotic process.

2.4 Fluorescein Diacetate Staining

An aliquot of 100 μL of unstained cell suspension (5 $\times 10^6$ cells/mL) was loaded on the picoliter well-per-cell array. Initial scanning was then performed in order to detect background scattering and auto-fluorescence. This undesired signal was recorded per measurement location and subtracted from the total emission signal (after staining) in order to obtain the correct fluorescence signal.

Cells were washed twice with incomplete RPMI 1640 medium without phenol red, containing 10 mM HEPES buffer solution. An aliquot of 100 μL of cell suspension (5 $\times 10^6$ cells/mL) was added to 50 μL of fluorescein diacetate staining solution (Sigma, St. Louis, MO, USA, F7378) in PBS, and incubated at room temperature for 5 min. At the end of incubation, cells were loaded onto the picoliter well-per-cell array (see the following explanation), washed three times with fresh buffer to remove excess staining solution, and measured.

Figure 1 shows (a) light and (b) fluorescent micrographs of the same individual living PBMC stained with fluorescein diacetate, positioned in the picoliter well-per-cell array. As it can be seen in Fig. 1, the diameter of cells, as observed by light and fluorescent microscopy, is the same. This signifies that the dye uniformly stains the entire cell.

Plasma membrane integrity of fluorescein diacetate stained cells was checked by re-staining the same cells with propidium iodide (PI). At the end of fluorescein diacetate measurement, the cells were washed twice with fresh buffer and a solution containing PI (2.5 μg/mL) was added on top of the pretested localized cells for 5 min. Cells were then washed twice and remeasured. Positive PI cells were excluded from the analysis.

To confirm apoptosis, Annexin V staining was performed. One million cells were washed with PBS and resuspended in binding buffer (Genzime, Cambridge, MA, USA). FITC Annexin V was added at a final concentration of 1 μg/mL. After

Fig. 2 Schematic representation of the FDTRM apparatus. The laser light passes through the Pockel cell and excites the sample. The Pockel cell and the detectors (PMT) are modulated by two frequency synthesizers and two RF amplifiers. All the data are collected by the personal computer controlling the entire measurement process (P— Polarizer).
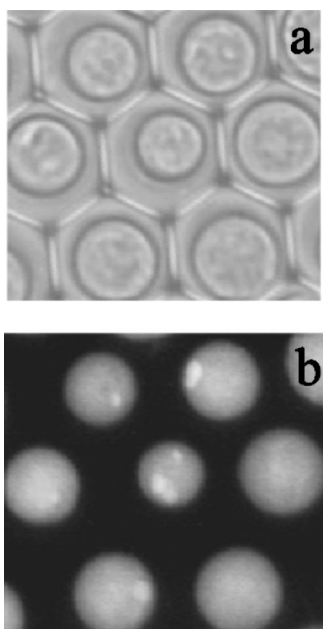
Fig. 1 (a) Light and (b) fluorescent micrographs of individual living PBMC, stained with fluorescein diacetate, positioned in the picoliter well-per-cell array.

10 min of incubation in the dark, at room temperature, cells were analyzed by FACS (Beckton-Dickenson, FACS-Calibur, Mountainview, CA, USA).

2.5 Measurement System

Measurements of FAD and τ_F were performed on live cells by microscopy, based on the frequency domain methodology.

Schematic depiction of the frequency domain time resolved microscope (FDTRM) is shown in Fig. 2. The FDTRM comprises two main stand-alone components: the optical system (an upright, epi-fluorescent Zeiss microscope Z-1) and a modified frequency domain FLT and FAD ISS K-2 spectrofluorimeter.

Briefly, an excitation of a 488 nm polarized beam from a continuous wave (cw) argon ionic laser (model 161B-070, Spectra-Physics, Mountain View, CA, USA) is directed to the light source entrance of the spectrofluorimeter, passing through an electro-optic Pockel's cell (Laser Metrics KD*P 1044, Winterpark, FL, USA) which modulates the beam at the frequency range from 1 kHz to 500 MHz. In most experiments, ten frequencies were used, ranging from 2 to 200 MHz in logarithmic scale. A small portion of the modulated excitation beam is sampled by a reference detector (Hamamatsu R928 PMT, Hamamatsu City, Japan), while the rest of it exits the spectrofluorimeter. Then it is doubly refracted by a mirror stirrer, impinges on the microscope illuminator (the epifluorescent arrangement) which directs the beam through the objective lens [×40, numerical aperture (NA)=0.60, LWD CD-Plan 40 PL, Olympus, Japan] that focuses the beam to, at most, a 15 μm diameter spot on the interrogation plane, where it illuminates the microscopic fluorescent sample under investigation. The Olympus objective was fitted to the Zeiss optical arrangement.
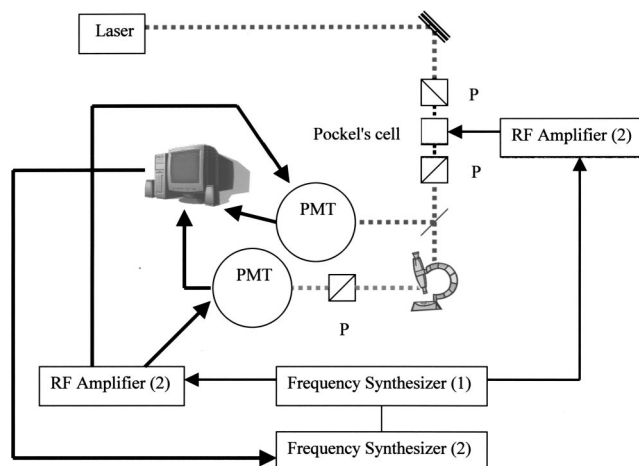
The diverging cone of the emitted fluorescence is then collected and collimated by the same objective, filtered by an emission filter (530±5 nm) and thereafter impinges on a Glan-Tomphson polarization analyzer, which splits the emission into two polarization (FA) components—parallel ($I_{\parallel}$) and orthogonal (I_{+}) emission field vectors—relative to the excitation field. Two modulated emission detectors (Hamamatsu R928 PMT) then simultaneously detect the 2 FA components, from which FAD can be calculated, as well as τ_R. For τ_F measurements, the same setup is used, but whereas one of the emission detectors is used for the measurement of the fluorescence signal, the other serves to measure the reference scattered excitation signal.

The induced photocurrent is then fed back to the ISS spectrofluorimeter electronic and computer units for calculation of the requested parameters. During measurements, the modulation frequency is changed automatically according to a predesigned menu. The integrated system is fully computer controlled. For FLT measurements, the polarizers of the system were configured to measure at the magic angle.

2.6 Individual Cell Measurement

50 μL of cell suspension are loaded on top of the specially designed picoliter well-per-cell array (Patent No. WO 03/035824). Single cells are then settled into the single cell wells (SCW) array by sedimentation. After sedimentation, the excess unsettled cells are washed out of the picoliter well-per-cell array. The bottom of a SCW possesses high optical quality. As a result, the transparent light image of a cell within a well can be recorded and correlated with its fluorescence signal. Each cell being held by a well, biological manipulations on the cell are possible (introduction of staining solutions, drugs, etc.) while preserving its identity. The excitation beam individually and sequentially illuminates the retained cells, and FLT and FAD of an individual fluorescent cell are measured.

Table 1 Steady state anisotropy of 10 μM fluorescein–glycerol solutions as measured by the FDTRM in two modes (steady-state and TRM) and the ISS-K2 spectrofluorimeter.

Measured solutions % glycerol in buffer aqua	Steady-state fluorescence anisotropy		
	ISS-K2	Steady state FDTRM	FDTRM
20%	0.047±0.037	0.054±0.01	0.058±0.025
40%	0.103±0.014	0.105±0.05	0.097±0.012
60%	0.120±0.026	0.121±0.013	0.118±0.009
80%	0.271±0.028	0.281±0.02	0.275±0.014

2.7 Data Analysis

The model function was represented by a sum of exponentials as shown in Eq. (2), where $I(t)$ is the fluorescence intensity at time t and α_i is the amplitude of the i'th lifetime τ_i, such that $\Sigma_i \alpha_i = 1$.

$I(t) = I_\parallel(t) + 2MI_+(t)$, and M is the microscope polarization correction factor which compensates for any optical and/or electrical distortion of the polarization components.

FAD was analyzed by the global fitting of $I_\parallel(t)$ and $I_+(t)$ to the following equations:

$$I_\parallel(t) = \tfrac{1}{3}I(t)[1 + 2r(t)],$$
$$I_+(t) = \tfrac{1}{3}I(t)[1 - r(t)]. \tag{4}$$

According to the assumed model, the fluorescent probes can be distributed between i hosting phases. The time-dependent anisotropy $r(t)$ is then represented as described by Eq. (2), where $r(t)$ is the FA at time t and β_j is the amplitude of the j'th rotational correlation time τ_{Rj}, such that $\Sigma_j \beta_j = r_0$.

The time resolved measurements were compared to steady state anisotropy (average over time) by utilizing both equalities in Eq. (2):

$$r = \frac{I_\parallel - MI_+}{I_\parallel + 2MI_+} = \frac{\int I(t)r(t)dt}{\int I(t)dt}$$
$$= \frac{\int \Sigma_{i,j} \alpha_i \exp(-t/\tau_{Fi})\beta_j \exp(-t/\tau_{Rj})dt}{\int \Sigma_i \alpha_i \exp(-t/\tau_{Fi})dt} \tag{5}$$

The quality of fits was evaluated by chi-square (χ^2) values based on weighted residuals.[6] A fit was considered to be within acceptable limits when $\chi^2 < 2$.

Decay curves of FI were analyzed by the standard multi-exponential MATLAB (MathWorks version 5.3 R11 Natick, MA, USA) fitting software and compared to ISS data analysis as well as to the software of the Center for Fluorescence Spectroscopy (CFS, University Maryland, College Park, MD, USA).

3 Results

3.1 System Performance Validation

All measurements were conducted at room temperature. Checkups and calibration runs of the entire system were performed daily, and included calculation of the relative modulation depth, phase shift, and the correction factor $M = I_\parallel/I_+$. The latter ratio was determined by measuring the FI of a nonviscose fluorescein solution. For all practical purposes, the measurements yield the M value of unity.

Calibration and validation runs were performed by comparing two types of measurements by two different systems (ISS-K2 and FDTRM) for the same sample: two steady-state FA measurements, and two TRM measurements. The TRM results were compared to the steady-state results using Eq. (5). For that purpose, 10 μM fluorescein-glycerol solutions with varying viscosities were measured. The results and their standard deviations (based on 10–50 repetitions) are listed in Table 1. They indicate a high level of correlation and thus the fitness of FDTRM.

3.2 Repeatability Test

The repeatability of the FDTRM performance was checked on fluorescent beads having 2000–50 000 MESF. One lifetime component equal to 4±0.1 ns was found. The FLT value of 4 ns for fluorescein is known to be as that in water solution (see Table 5, row 1, and Refs. 7 and 8), i.e., the dye labeling the beads experiences the same environmental conditions as in water solution. In addition, in FAD measurements (more than 50 measurements were conducted), only one component of τ_R equal to 3.1±0.85 ns was observed.

Computation of the steady state FA via Eq. (5), utilizing the measured values of τ_F and τ_R, yielded $r = 0.18 \pm 0.02$, in agreement with the steady state FA measured by both systems: the ISS-K2 and the FDTRM in a steady state mode.

3.3 Measurements of FLT and FAD in Cellular Models

Two cellular models were considered: the mitogenic stimulation of peripheral blood mononuclear cells (PBMC), and apoptosis induction in Jurkat T cells (JTC). Previous studies[9–11] have indicated that in mitogenic activation the steady state FA

Table 2 Measurements of FLT and FAD in individual cells incubated with (A_s) and without (A_0) PHA.*

State	τ (ns)	β	τ_R (ns)	r	r steady-state mode
A_0	4±0.05	0.4±0.08	2.5±0.09	0.153±0.02	0.158±0.008
A_s	4.5±0.11	0.39±0.07	2±0.25	0.123±0.03	0.12±0.01

* The steady-state FA was calculated and compared to the steady-state mode of FDTRM and ISS-K2 apparatuses (r steady state mode: average by the two systems).

Table 3 FLT and FAD as measured by FDTRM in individual cells at $t=0$ (A_0) and $t=180$ min $(A_{\mathrm{H_2O_2}})$ after the onset of apoptosis.

State	τ (ns)	β	τ_R (ns)	r	r steady-state mode
A_0	4.1 ± 0.1	0.4 ± 0.05	2.1 ± 0.09	0.135 ± 0.04	0.135 ± 0.015
$A_{\mathrm{H_2O_2}}$	4.05 ± 0.25	0.395 ± 0.08	3.3 ± 0.3	0.177 ± 0.03	0.17 ± 0.02

decreases, whereas in apoptosis the FA increases. These two findings were the main reason for choosing these models for the present study.

3.3.1 Monitoring of mitogenic stimulation in PBMC via FA

Table 2 shows the measured FLT and FAD of fluorescein diacetate stained PBMC, treated with the mitogen PHA (defined as A_s condition) or untreated (defined as A_0 condition). As it can be seen, following mitogenic stimulation, the steady-state FA (r) decreases. In addition, the marker's FLT increases by more than 12%, from 4 ± 0.05 ns in untreated cells to 4.5 ± 0.11 ns in cells incubated with PHA. Moreover, measurement of the rotational correlation time clearly indicates that there exists only one decaying component with τ_R decreasing by 20%, from 2.5 ± 0.09 (in untreated cells) to 2 ± 0.25 ns in PHA treated cells. In agreement with Eq. (1), this behavior of τ_F and τ_R explains the decrease in the steady state FA following mitogenic stimulation of fluorescein diacetate stained cells.

3.3.2 Monitoring of apoptosis in Jurkat T cells via FA

The FLT and FAD were measured in fluorescein diacetate stained JTC, either untreated or treated for apoptosis induction for 3 h with 50 μM H_2O_2. The results, presented in Table 3, show that τ_F values in apoptotic Jurkat T cells are similar to those of untreated cells (4.1 ns). However, τ_R increases from 2.1 ± 0.09 in untreated cells to 3.3 ± 0.3 ns in cells in which apoptosis was induced. The apoptotic process was confirmed by measuring the steady state FA and by Annexin staining.[11]

Contrary to the mitogenic stimulation described previously, in the apoptotic model, changes in the steady-state FA seem to be due to changes in the rotational correlation time rather than FLT.

3.4 Complementary Experiments

Generally, cellular events involve several chemo-physical alterations that may affect the steady-state FA. Among these are pH, viscosity, polarity, concentrations of various intracellular ions, etc.[8,12] In the following experiments we investigated the possibility of a direct influence of some of the above variables upon the FLT and FAD of a hosted probe.

3.4.1 FLT and FAD dependence on pH

It might be suspected that changes in steady-state FA only reflect a variation in pH occurring during cell activation.[13] To examine the dependence of FLT and FAD on pH, four solutions of fluorescein (2 μM)-glycerol (40%) in PBS were prepared, having pH values of 5, 6.5, 7.4, and 8.

In all measurements, only one lifetime and one rotational correlation time component were found in both ISS-K2 and FDTRM systems. Further, the results by both apparatuses were similar (Table 4). By the FDTRM, τ_F, τ_R, and r_0 were found to be 3.78 ± 0.1 ns, 1.38 ± 0.3 ns and 0.37 ± 0.02, respectively, whereas with the ISS-K2 system they were 3.8 ± 0.2 ns, 1.3 ± 0.42 ns, and 0.38 ± 0.1, for all pH values. Applying Eq. (5) to these results, the steady-state FA was calculated and found to be 0.108 ± 0.001, similar to the directly measured value (Table 1, second row).

3.4.2 FLT and FAD dependence on viscosity

One of the effects of viscosity upon fluorescein is the shortening of its fluorescence decay time.[13] We examined the possibility that the shortening of FLT as a function of η might enhance the obvious dependence of r on η. Four fluorescein (2 μM) solutions with different glycerol concentrations in PBS (0, 30%, 60%, and 80%) were prepared, all having pH value of 7.4.

The results shown in Table 5 indicate a strong dependence of FLT on glycerol concentration (a decrease from 4.01 ns at

Table 4 Dependence of FLT and FAD on pH.*

	FDTRM				ISS-K2			
pH	τ (ns)	τ_R (ns)	r_0	FA	τ (ns)	τ_R (ns)	r_0	FA
5	3.78 ± 0.1	1.38 ± 0.3	0.37 ± 0.02	0.098 ± 0.08	3.8 ± 0.2	1.5 ± 0.6	0.36 ± 0.05	0.101 ± 0.03
6.5	3.7 ± 0.15	1.4 ± 0.35	0.365 ± 0.06	0.1 ± 0.002	3.82 ± 0.25	1.55 ± 0.3	0.37 ± 0.08	0.106 ± 0.07
7.4	3.69 ± 0.18	1.3 ± 0.25	0.375 ± 0.08	0.097 ± 0.06	3.85 ± 0.23	1.65 ± 0.25	0.36 ± 0.15	0.108 ± 0.001
8	3.8 ± 0.08	1.37 ± 0.29	0.37 ± 0.04	0.098 ± 0.004	3.78 ± 0.32	1.52 ± 0.55	0.38 ± 0.1	0.108 ± 0.09

* FLT and FAD of fluorescein in 40% glycerol solutions, having pH levels of 5, 6.5, 7.4, and 8, were measured by the FDTRM and ISS-K2. $\chi^2 < 1.48$.

Table 5 Influence of viscosity on FLT and FAD in 2 μM fluorescein solutions at pH=7.4.*

% Gly	Lifetime τ (ns)	Anisotropy decay			
		β	τ_R (ns)	r	r_0
0	4.014±0.2	0.4 ±0.1	0.5±0.09	0.04	0.4
30	3.85 ±0.35	0.37±0.15	1.5±0.17	0.1	0.37
60	3.7 ±0.17	0.33±0.09	2.2±0.3	0.12	0.33
80	3.6 ±0.1	0.3 ±0.11	35 ±5.4	0.27	0.3

* Viscosity was altered by changing glycerol concentrations. $\chi^2 < 1.429$.

Fig. 3 FLT and FA of 10 μM fluorescein in 80% glycerol solution with different H_2O_2 concentrations. The full line indicates the FA (right scale) and the dashed line indicates the FLT (left scale). The abscissa scale indicating the H_2O_2 concentrations is drawn logarithmically.

0% Gly to 3.6 ns at 80% Gly), and an increase of calculated r value from 0.04 to 0.27, correspondingly (the latter value is similar to that obtained by direct r steady state measurements, see Table 1, last row). These results are in agreement with recent publications.[14] Measurements of FAD show an even greater dependence on glycerol concentration, an increase of τ_R from 0.5 to 35 ns, correspondingly.

We further examined the cause of FLT decrease, namely, whether it depends on viscosity changes or interaction with glycerol molecules. To test this, FLT of three fluorescein (2 μM) glycerol solutions in PBS (0, 40%, and 60%) were measured at the temperature range from 15 to 30 °C. The pH levels of the solutions were 6.12, 7.3, and 8.3. The results, shown in Table 6, indicate almost no change in FLT, whereas the steady-state FA clearly decreases. This signifies that FAD is the dominant parameter affecting the steady-state FA. Further, glycerol seems to alter the fluorescein molecule conformation or the angle between the absorption and emission dipole moments as evidenced by the changes in r_0 values listed in Table 5.

3.4.3 *FLT dependence on H_2O_2*

One of the best-known collisional quenchers of fluorescence is molecular oxygen, a product of H_2O_2. Hence, in the pres-

ence of H_2O_2, FLT might be changed, and consequently FA may change as well.[6] In order to negate the possibility that during H_2O_2 apoptosis induction the measured fluorescence characteristics were directly influenced by the presence of H_2O_2 and/or its products, the following experiment was preformed in cell free solutions with known viscosity. Fluorescein (10 μM) glycerol (80%) solutions, in the presence of different concentrations of H_2O_2 (0, 50, 1000, and 16 000 μM) were prepared and FA and FLT were measured.

The results are shown in Fig. 3. The FLT did not change for the H_2O_2 range of 0–16 000 μM, and remained at the value of 3.6±0.15 ns. However, FA increased by more than 10% from 0.28±0.05 at 0 μM, to 0.312±0.06 at 16 000 μM H_2O_2, which indicates that FA is not influenced by FLT.

4 Discussion

The present study offers FLT and FAD measurements as differential indicators of cellular activity.

The combination of the frequency mode time resolved measurements and the picoliter well-per-cell array is designed to allow FLT and FAD measurements in individual cells under varying biological conditions. There are three considerable advantages to the suggested combined methodology. First, the analysis of fluorescence decay is self-referential since the

Table 6 Dependence of FLT and FAD on glycerol concentrations and temperature.

Gly %	T (°C)	pH=8.3		pH=7.3		pH=6.12	
		τ (ns)	r	τ (ns)	r	τ (ns)	r
0%	15.5	—	—	4.171	0.026	—	—
	29.6	—	—	4.183	0.016	—	—
40%	16	3.968	0.076	3.935	0.082	3.87	0.085
	20.3	3.962	0.07	3.959	0.073	3.87	0.076
	24	3.975	0.064	3.953	0.066	3.865	0.065
	29.4	3.988	0.05	3.958	0.054	3.863	0.054
60%	16	—	—	3.798	0.181	—	—
	29.7	—	—	3.834	0.127	—	—

characteristics of the decay are indicated by the way in which the fluorescence intensity of the sample decreases relative to its intensities at earlier time points. The second is the ability to characterize a nonadhesive and heterogeneous population, based on functional time resolved parameters. The third advantage lies in the measured parameters themselves. In addition to their bioactivity indicative capacity, FLT, FAD, r_0 and β_∞ may provide valuable information about cellular mechanisms that may involve complex molecular diffusion dynamics, as well as information about structural changes which the reporter molecule experiences in the course of cell activation.

The exemplary experimental models of this study demonstrate these capabilities. Stimulation of PBMC with PHA was found to alter both the FLT (from 4 ± 0.05 before to 4.5 ± 0.11 ns after stimulation) and FAD (2.5 ± 0.09 and 2 ± 0.25 ns, correspondingly) of intracellular fluorescein (see Table 2). In stimulated PBMC, both parameters change, meaning that not only the viscous environment changed, but the fluorescein molecular quantum parameters changed as well. In other cases, only changes in viscosity affect the FA. The experiment on JTC gives evidence that the FAD is the dominant determinative parameter and not the FLT. In JTC undergoing H_2O_2 induced apoptosis, only FAD changed (from 2.1 ± 0.09 ns at $t=0$ after the treatment with H_2O_2 to 3.3 ± 0.3 ns at $t=180$ min) and the FLT remained constant (4.1 ns)—see Table 3. This finding is supported by the fact that, in fluorescein solutions, the same behavior is observed (Fig. 3). When measuring fluorescein in low viscosity buffer, the steady-state FA is low (0.04 in 20% glycerol solution—Table 1), and in a more viscous solution the steady-state FA is high (0.281 in 80% glycerol solution—Table 1). The reason for the difference is not the FLT, which remained unchanged in solutions with different viscosity (3.9 ns in 40% glycerol—Table 6), but the FAD which was changed. In solutions with low viscosity, the FAD is very short, whereas in the more viscous solution the FAD is much longer (Table 5).

High FA values in cells may point out to a significant restriction of the probe mobility, imposed by its intracellular microenvironment. There may be several causes for such restriction: structural, e.g., caging and "wobbling-in-cone,"[15] binding properties (covalent bonding, dipole–dipole interactions, or interactions of higher orders of charge arrangement), or simply the solvent viscosity. The present results indicate that the FA alterations during stimulation and apoptotic process may appear due to both the FLT and fluorescence correlation time changes, and in some cases due to the fluorescence correlation time rather than FLT (FLT is indicative of changes in the fluorescence quantum state). The same interpretation can be made of our previous findings that indicated a clear correlation with respect to FA between the processes of PBMC response to mitogens,[16] as well as to antigens[17] and phorobol esters,[18] the interaction between killer and target cells,[8] and the contraction cycle of cardiac cells[10]—in all, the FA decreases during 20 min following the stimulation/conjugation.

In addition to the FLT and the rotational correlation time, there are two other parameters which may determine FAD. The first is r_0, which is in fact the FA limiting value. The second parameter is β_∞ which indicates that even at the time$\rightarrow\infty$, FA differs from 0. The r_0 indicates an intramolecular structural aspect, i.e., the angle between the absorption and emission transition dipole moments. A change in r_0 of a fluorescent solute reporter hosted in a live cell, may reflect the micro-environmental forces acting on the reporter under different intracellular physiological conditions.

In the present study, r_0 of fluorescein was changed from 0.4 to 0.3 when dissolved in 0% glycerol and 80% glycerol solutions, respectively (Table 5). Our results for fluorescein in nonviscous solutions are in agreement with previous studies.[19] Lowering of the viscosity of fluorescein–glycerol solution by mild heating decreased the FA (Table 6), which is exponentially dependent on temperature, after Andrade[20] and others,[12] but did not alter r_0. Since the gentle heating does not alter the glycerol concentration, the fluorescent probe should experience, on the average, the same amount of influence by glycerol molecules. This may suggest that the decrease of r_0 from 0.4 to 0.3, indicative of conformational changes, may be due to glycerol–fluorophore interaction rather than to the viscosity per se.

References

1. H. M. Shapiro, *Practical Cytometry*, pp. 314, 315, and 327–329, Alan R. Liss Inc., New York (1995).
2. J. Alberola-Ila, S. Takaki, J. D. Kerner, and R. M. Perlmutter, "Differential signaling by lymphocyte antigen receptors," *Annu. Rev. Immunol.* **15**, 125–154 (1997).
3. M. Van Graft, Y. M. Kraan, I. M. Segers, K. Radosevic, B. G. De Grooth, and J. Greve, "Flow cytometric measurement of [Ca2+]i and pHi in conjugated natural killer cells and K562 target cells during the cytotoxic process," *Cytometry* **14**, 257–264 (1993).
4. F. Perrin, "Polarisation de la lumiere de fluorescence. Vie moyenne des molecules dans l'etat excite," *J. de Physique, VIe serie* **7**, 390–401 (1926).
5. A. Jablonski, "On the notion of the emission anisotropy," *Bull. Acad. Pol. Sci., Ser. Sci., Math., Astron. Phys.* **8**, 259–264 (1960).
6. J. R. Lakowicz, *Principles of Fluorescence Spectroscopy*, 2nd ed., pp. 145–146 and 237–264, Kluwer Academic Plenum Publishers, New York (1999).
7. R. Sjöback, J. Nygren, and M. Kubista, "Absorption and fluorescence properties of fluorescein," *Spectrochim. Acta, Part A* **51**, L7–L21 (1995).
8. D. Fixler, R. Tirosh, A. Eisenthal, S. Lalchuk, O. Marder, and M. Deutsch, "Prelytic stimulation of target and effector cells following conjugation as measured by intracellular fluorescein fluorescence polarization," *J. Biomed. Opt.* **3**, 312–325 (1998).
9. N. Zurgil, M. Deutsch, R. Tirosh, and C. Brodie, "Indication that intracellular fluorescence polarization of T lymphocytes is cell cycle dependent," *Cell Struct. Funct* **21**, 271–276 (1996).
10. N. Zurgil, Z. Schiffer, Y. Shafran, M. Kaufman, and M. Deutsch, "Fluorescein fluorescence hyperpolarization as an early kinetic measure of the apoptotic process," *Biochem. Biophys. Res. Commun.* **268**, 155–163 (2000).
11. N. Zurgil, Y. Shafran, D. Fixler, and M. Deutsch, "Analysis of early apoptotic events in individual cells utilizing fluorescence intensity and polarization measurements," *Biochem. Biophys. Res. Commun.* **290**, 1573–1582 (2002).
12. D. Fixler, R. Tirosh, A. Shainberg, and M. Deutsch, "Cytoplasmic changes in cardiac cells during contraction cycle detected by fluorescence polarization," *J. Fluoresc.* **11**, 89–100 (2001).
13. P. P. Feofilov, *The Physical Basis of Polarized Emission*, Consultants Bureau, New York (1961).
14. A. H. Clayton, Q. S. Hanley, D. J. Arndt-Jovin, V. Subramaniam, and T. M. Jovin, "Dynamic fluorescence anisotropy imaging microscopy in the frequency domain (rFLIM)," *Biophys. J.* **83**, 1631–1649 (2002).

15. G. Lipari and A. Szabo, "Effect of librational motion on fluorescence depolarization and nuclear magnetic resonance relaxation in macro-molecules and membranes," *Biophys. J.* **30**, 489–506 (1980).

16. A. Eisenthal, O. Marder, D. Dotan, S. Baron, B. Lifschitz-Mercer, S. Chaitchik, R. Tirosh, A. Weinreb, and M. Deutsch, "Decrease of intracellular fluorescein fluorescence polarization (IFFP) in human peripheral blood lymphocytes undergoing stimulation with phyto-haemagglutinin (PHA), concanavalin A (ConA), pokeweed mitogen (PWM) and anti-CD3 antibody," *Biol. Cell* **86**, 145–150 (1996).

17. H. Rahmani, M. Deutsch, I. Ron, S. Gerbat, R. Tirosh, A. Weinreb, S. Chaitchik, and S. Lalchuk, "Adaptation of the cellscan technique for the SCM test in breast cancer," *Eur. J. Cancer* **32A**, 1758–1765 (1996).

18. A. Eisenthal, O. Marder, B. Lifschitz-Mercer, Y. Skornick, R. Tirosh, A. Weinreb, and M. Deutsch, "Inhibition of mitogen-induced changes in intracellular fluorescein fluorescence polarization of hu-man peripheral blood lymphocytes by colchicine, vinblastine and cy-tochalasin B," *Cell Struct. Funct* **21**, 159–66 (1996).

19. L. Szalay, L. Gati, and B. Sarkany, "On the fundamental polarization of the fluorescence of viscous solutions," *Acta Phys. Acad. Sci. Hung* **14**, 217–224 (1962).

20. E. N. da C. Andrade, "The viscosity of liquids," *Endeavour* **12**, 117–127 (1954).